

Complex Trajectories in the Quartic Oscillator and Its Semiclassical Coherent-State Propagator

Ademir L. Xavier Jr. and Marcus A. M. de Aguiar

*Departamento de Física do Estado Sólido e Ciência dos Materiais,
Universidade Estadual de Campinas, CP 6165, Campinas, Brazil*

Received April 3, 1996

The semiclassical approximation of the coherent-state propagator requires the computation of complex trajectories satisfying special boundary conditions. In this paper we present a method for the determination of such trajectories for one-dimensional polynomial potentials. We also compute the semiclassical propagator for the case $V(q) = \lambda q^2/2 + \beta q^4$ and compare the results with an “exact” calculation. © 1996 Academic Press, Inc.

1. INTRODUCTION

The semiclassical limit of quantum theory has attracted the attention of physicists since its inception. The definition of “tunneling time” and the exact way classical chaos is recovered from quantum mechanics are examples of questions that remain open. Among the several developments occurred in the past 30 years, there is the semiclassical theory for the coherent-state propagator, given by

$$K(z'', z', T) = \langle z'' | e^{-iHT/\hbar} | z' \rangle,$$

where $|z\rangle$ is the harmonic oscillator coherent-state (see next section for a precise definition). The study of the dynamical evolution of $|z', t\rangle$ is attractive because it represents the time evolution of what most closely approximates a classical point in phase space, that is, a Gaussian distribution with minimum uncertainty. The coherent-state propagator represents the probability amplitude of the time evolved wave-packet to be another coherent-state at z'' . If the classical dynamics does not affect significantly the shape of the initial packet, we expect to find large amplitudes for the state $|z''\rangle$ whose center corresponds to the classically evolved center of $|z'\rangle$, according to Ehrenfest’s theorem.

A semiclassical formula for $K(z'', z', T)$ can be obtained with the help of the path-integral formulation [1–3]. It turns out that, in the limit $\hbar \rightarrow 0$, $K(z'', z', T)$ can be written in terms of classical trajectories only, similarly to the usual coordinate propagator $\langle x'' | e^{-iHT/\hbar} | x' \rangle$, with the difference that the trajectories contributing to $K(z'', z', T)$ are generally complex, although T remains a real parameter, even in presence of tunnelling. In particular this method is suitable for problems lacking

usual (real) trajectories in phase space. Several schemes of complexification have been recently studied [4–6], aiming at an improvement in the semiclassical description in these particular regions. Some of these schemes, however, treat the time as a complex variable, which turns out to be difficult to interpret physically.

In a recent paper [7] we studied in detail the one-dimensional problem of a particle in a box. Although the complexification of phase space required by the semiclassical theory turns the problem into a two-dimensional effective problem, the simplicity of the Hamiltonian still allowed for an analytical solution of the semiclassical propagator. In this paper we deal with the more generic situation of smooth one-dimensional Hamiltonians. We present a numerical method based upon the monodromy method [8], that allows the complete determination of the complex trajectories within the context of the semiclassical approximation to the coherent-state propagators [9] in which the time is a real variable. We apply the method to the quartic Hamiltonian ($\lambda > 0$, $\beta > 0$)

$$H = \frac{1}{2} p^2 + \frac{\lambda}{2} q^2 + \beta q^4,$$

and compute the exact and semiclassical propagators, comparing results.

This paper is organized as follows: in Section 2 we review the main semiclassical formulas; in Section 3 we present the numerical algorithm to compute the complex trajectories; in Section 4 we apply the method to the quartic Hamiltonian, computing trajectories as well as the propagators. Section 5 is devoted to the conclusions.

2. COMPLEX ORBITS AND THE SEMICLASSICAL PROPAGATOR

The coherent-state propagator is defined by

$$K(z'', z', T) = \langle z'' | e^{-i\hat{H}T/\hbar} | z' \rangle, \quad (1)$$

where

$$|z\rangle = e^{-1/2 |z|^2} e^{za^\dagger} |0\rangle \quad (2)$$

is the harmonic oscillator coherent-state, $|0\rangle$ is the ground state and

$$a^\dagger = \frac{1}{\sqrt{2}} \left(\frac{\hat{q}}{b} + i \frac{\hat{p}}{c} \right), \quad z = \frac{1}{\sqrt{2}} \left(\frac{q}{b} + i \frac{p}{c} \right), \quad (3)$$

with $bc = \hbar$. In (3) the parameters q and p are real numbers corresponding to the average value of the operators \hat{q} and \hat{p} . In Ref. [9] a semiclassical approximation for (1) was obtained by writing (1) as a path-integral and solving it by the steepest descent method [10]. The result is that $K(z'', z', T)$ can be written as a sum over

contributions (see Eqs. (7) and (8) below) from complex trajectories obeying the equations

$$ih\dot{u} = \frac{\partial H}{\partial v}, \quad ih\dot{v} = -\frac{\partial H}{\partial u}, \quad (4)$$

with

$$u = \frac{1}{\sqrt{2}} \left(\frac{q}{b} + i \frac{p}{c} \right), \quad v = \frac{1}{\sqrt{2}} \left(\frac{q}{b} - i \frac{p}{c} \right), \quad (5)$$

and special boundary conditions

$$u(0) \equiv \frac{1}{\sqrt{2}} \left(\frac{q'}{b} + i \frac{p'}{c} \right) \equiv u' = z', \quad v(T) \equiv \frac{1}{\sqrt{2}} \left(\frac{q''}{b} - i \frac{p''}{c} \right) \equiv v'' = z''^*. \quad (6)$$

The new variables u and v are independent complex numbers not necessarily complex conjugate of each other. This means that q and p are themselves complex variables. As explained in [7, 9], such extension to a complex phase space is indeed necessary, and it comes out naturally from the steepest descent approximation. In (4) H is the classical Hamiltonian obtained by substituting the inverse of the transformation (5) into $H(q, p)$. The final semiclassical formula for (1) reads

$$K_{sc}(z'', z', T) = \sum_j \sqrt{\frac{i}{\hbar} \frac{\partial^2 S_j}{\partial u' \partial v''}} \exp \left[\frac{i}{\hbar} S_j(v'', u', T) - \frac{1}{2} (|v''|^2 + |u'|^2) \right], \quad (7)$$

with

$$S_j(v'', u', T) = \int_0^T \left[\frac{i\hbar}{2} (v_j \dot{u}_j - \dot{v}_j u_j) - H(u_j, v_j) \right] dt - \frac{i\hbar}{2} (v'' u_j'' + u' v_j') \quad (8)$$

being the *complex* action of the j th trajectory. The sum over j in (7) is performed over all possible (complex) classical trajectories compatible with the conditions (6). The function S obeys the relations

$$-ihu' = \frac{\partial S}{\partial v''}, \quad -ihv' = \frac{\partial S}{\partial u'}, \quad -H = \frac{\partial S}{\partial T}. \quad (9)$$

Similar to S the new Hamiltonian H is a complex function, and it is convenient to write both these functions in terms of real and imaginary parts as $S = S_1 + iS_2$ and $H = H_1 + iH_2$. In the special case where $S_2 = 0$ and $H_2 = 0$, then, for all times t , we have

$$u(t) = v^*(t), \quad (10)$$

and the trajectory is real.

In this paper we shall be mainly concerned with the development of a special numerical method for the determination of general solutions of (4) and, consequently, the numerical determination of (8). For the sake of simplicity we shall present our method for systems with one degree of freedom only, i.e., systems whose complex versions have two freedoms. The generalization for any number of freedoms is straightforward [9].

Let us define new real variables x_1, x_2, p_1 and p_2 , so that

$$\begin{aligned} q &= x_1 + ip_2, \\ p &= p_1 + ix_2, \end{aligned} \tag{11}$$

then Eqs. (4) become

$$\begin{aligned} \dot{x}_1 &= \frac{1}{2} \left(\frac{\partial H_1}{\partial p_1} + \frac{\partial H_2}{\partial x_2} \right), & \dot{p}_1 &= -\frac{1}{2} \left(\frac{\partial H_1}{\partial x_1} + \frac{\partial H_2}{\partial p_2} \right), \\ \dot{x}_2 &= \frac{1}{2} \left(\frac{\partial H_1}{\partial p_2} - \frac{\partial H_2}{\partial x_1} \right), & \dot{p}_2 &= -\frac{1}{2} \left(\frac{\partial H_1}{\partial x_2} - \frac{\partial H_2}{\partial p_1} \right). \end{aligned} \tag{12}$$

If now we restrict H to *analytic* functions only, which does not imply any serious loss at all, we can rewrite these equations in terms of the real part of H only

$$\begin{aligned} \dot{x}_1 &= \frac{\partial H_1}{\partial p_1}, & \dot{p}_1 &= -\frac{\partial H_1}{\partial x_1}, \\ \dot{x}_2 &= \frac{\partial H_1}{\partial p_2}, & \dot{p}_2 &= -\frac{\partial H_1}{\partial x_2}. \end{aligned} \tag{13}$$

Equations (13) are the usual Hamilton's equations for a 2-degree of freedom system.

Most of the Hamiltonians of interest are analytic, specially the polynomial potentials

$$H = \frac{1}{2} p^2 + \sum_{j=1}^N q_j q^j. \tag{14}$$

Nevertheless the particle in a box [7] is an example where a non-analytic Hamiltonian system was treated by Eq. (13). In this case, however, the Hamiltonian function is seen as the limit of a polynomial potential of large degree,

$$H_{inf.well} = \frac{1}{2} p^2 + \lim_{n \rightarrow \infty} \left\{ \left(\frac{2q}{L} \right)^{2n} \right\}, \tag{15}$$

with L the size of the one-dimensional box.

Finally the boundary conditions (6) in the new coordinate system are given by

$$\begin{aligned}x_1(0) &= -\frac{b}{c}x_2(0) = q', \\x_1(T) + \frac{b}{c}x_2(T) &= q'', \\p_1(0) + \frac{c}{b}p_2(0) &= p', \\p_1(T) &= \frac{c}{b}p_2(T) = p''.\end{aligned}\tag{16}$$

3. NUMERICAL ALGORITHM

The numerical method described here follows very closely the monodromy matrix method developed by M. Baranger *et al.* [8] to compute periodic orbits. Given an initial tentative orbit, the method iterates this initial guess for a number of times according to the linearized dynamics of the system, as in the usual Newton's method. The iteration session ends when the final corrected trajectory satisfies Eq. (13) with a given accuracy. The initial tentative trajectory should necessarily obey conditions (16), which remain unchanged during the iteration process.

In terms of the phase space vector $r = (x_1, x_2, p_1, p_2)$, Eq. (13) can be written in the following compact form (summation convention)

$$\dot{r}_j = \mathcal{J}_{jk} \frac{\partial H_1(r_i)}{\partial r_k},\tag{17}$$

with \mathcal{J}_{jk} given by

$$\mathcal{J} = \begin{pmatrix} 0 & 0 & -1 & 0 \\ 0 & 0 & 0 & -1 \\ 1 & 0 & 0 & 0 \\ 0 & 1 & 0 & 0 \end{pmatrix}.\tag{18}$$

Dividing the time interval T into $(N-1)$ equal parts of size $\varepsilon = T/(N-1)$, Eq. (17) assumes the discrete form

$$r_j^{(n+1)} = r_j^{(n)} + \varepsilon \mathcal{J}_{jk} \frac{\partial H_1[\bar{r}_j^{(n)}]}{\partial r_k},\tag{19}$$

where $\bar{r}^{(n)} = \frac{1}{2}(r^{(n+1)} + r^{(n)})$ and $r_i^{(n)} = r_i(n\varepsilon)$. Assuming that an initial guess $r_i^{(n)}$, $n = 1, 2, \dots, N$ satisfying conditions (16) is available, we compute a correction $\Delta r_i^{(n)}$ by imposing that $r_i^{(n)} + \Delta r_i^{(n)}$ satisfies (19) to first order in $\Delta r_i^{(n)}$. Using

$$\frac{\partial H_1[r_i^{(n)} + \Delta r_i^{(n)}]}{\partial r_k} \simeq \frac{\partial H_1[r^{(n)}]}{\partial r_k} + \frac{\partial^2 H_1[r^{(n)}]}{\partial r_l \partial r_k} \Delta r_l^{(n)}, \tag{20}$$

we find that $\Delta r^{(n)}$ must satisfy

$$V^{(n)} \Delta r^{(n+1)} = \mathcal{U}^{(n)} \Delta r^{(n)} + \mathcal{R}^{(n)}, \tag{21}$$

where

$$\mathcal{R}_j^{(n)} = -(r_j^{(n+1)} - r_j^{(n)}) + \varepsilon \mathcal{J}_{jk} \frac{\partial H_1[\bar{r}^{(n)}]}{\partial r_k}, \tag{22}$$

$$V_{jl}^{(n)} = \delta_{jl} - \frac{\varepsilon}{2} \mathcal{J}_{jk} \frac{\partial^2 H_2[\bar{r}^{(n)}]}{\partial r_l \partial r_k}, \tag{23}$$

and

$$\mathcal{U}_{jl}^{(n)} = \delta_{jl} + \frac{\varepsilon}{2} \mathcal{J}_{jk} \frac{\partial^2 H_1[\bar{r}^{(n)}]}{\partial r_l \partial r_k}. \tag{24}$$

Multiplying both sides of (21) by $[V^{(n)}]^{-1}$, and using this equation recursively starting from $\Delta r^{(0)}$, gives

$$\Delta r^{(N+1)} = \mathcal{M} \Delta r^{(0)} + \mathcal{B}, \tag{25}$$

where

$$\mathcal{B} = \sum_{l=1}^{N-1} \left[\prod_{k=l+1}^N (V^{-1} \mathcal{U})^{(k)} \right] V^{-1^{(l)}} \mathcal{R}^{(l)} + V^{-1^{(0)}} \mathcal{R}^{(0)}, \tag{26}$$

and

$$\mathcal{M} = \prod_{m=0}^N (V^{-1} \mathcal{U})^{(m)}. \tag{27}$$

Here \mathcal{M} plays the role of monodromy matrix for the non-closed trajectory.

We finally connect $\Delta r^{(N+1)}$ to $\Delta r^{(0)}$ by imposing the boundary conditions. Relations (16) imply that

$$\begin{aligned}
 \Delta x_1(0) &= \frac{b}{c} \Delta x_2(0), \\
 \Delta p_1(0) &= -\frac{c}{b} \Delta p_2(0), \\
 \Delta x_1(T) &= -\frac{b}{c} \Delta x_2(T), \\
 \Delta p_1(T) &= \frac{c}{b} \Delta p_2(T),
 \end{aligned} \tag{28}$$

and the initial and final corrections can be expressed in terms of a single 4-vector W_1 by

$$\Delta r^{(0)} = \begin{pmatrix} 1 & 0 & 0 & 0 \\ c/b & 0 & 0 & 0 \\ 0 & 0 & 1 & 0 \\ 0 & 0 & -b/c & 0 \end{pmatrix} \begin{pmatrix} \Delta x_1(0) \\ \Delta x_1(T) \\ \Delta p_1(0) \\ \Delta p_1(T) \end{pmatrix} \equiv A_0 W_1, \tag{29}$$

and

$$\Delta r^{(N+1)} = \begin{pmatrix} 0 & 1 & 0 & 0 \\ 0 & -c/b & 0 & 0 \\ 0 & 0 & 0 & 1 \\ 0 & 0 & 0 & b/c \end{pmatrix} \begin{pmatrix} \Delta x_1(0) \\ \Delta x_1(T) \\ \Delta p_1(0) \\ \Delta p_1(T) \end{pmatrix} \equiv A_N W_1. \tag{30}$$

Substituting (29) and (30) back into (25), we finally have

$$\begin{aligned}
 W_1 &= (A_0 - \mathcal{M} A_N)^{-1} \mathcal{B}, \\
 \Delta r^{(0)} &= A_0 (A_0 - \mathcal{M} A_N)^{-1} \mathcal{B},
 \end{aligned} \tag{31}$$

which, together with Eq. (25), determine the correction for the whole orbit. The whole process is then iterated until the desired precision.

The convergence of the method is guaranteed provided the initial tentative trajectory is sufficiently close to the solution. The convergence velocity depends also naturally on the distance of the initial guess from the final solution. In some cases there are more than one trajectory satisfying the same boundary conditions and, depending on the initial guess, the above algorithm will converge to one or another of these trajectories. As we will see, for general potentials of the form (14), in order to obtain complex trajectories, real orbits may be used as initial tentative trajectories. For the computation of diagonal elements $z'' = z'$ of the propagator (1), for example, the real orbits are necessarily periodic. In the case of the quartic well, for

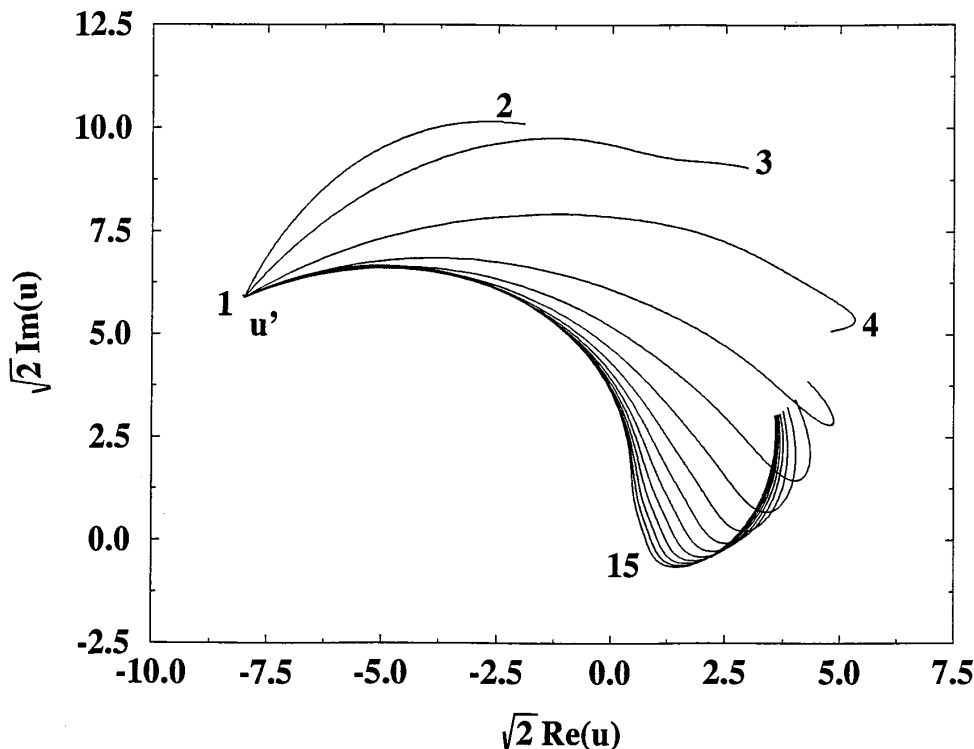


FIG. 1. Sequence of non-diagonal complex trajectories in the $\sqrt{2} \text{Re}(u) - \sqrt{2} \text{Im}(u)$ plane for $q' = -8.0$, $q'' = 0.0$, $p' = 5.9$, $p'' = 7.9$, and $M = 15$ between the times $T_0 = 0.001$ and $T_F = 4.5$. The numbers on Figs. 1-5 represent the value of j in Eq. (39) ($\lambda = 0$, $\beta = 0.2$).

instance, for a given point (q, p) in phase space, there is in general no periodic orbit corresponding to the time T . However, there is a periodic orbit with period $\tau(q, p)$, and this is the orbit that enters the algorithm as the tentative trajectory. In this way real orbits constitute the skeleton upon which complex solutions in phase space can be built.

The complete determination of the semiclassical propagator (7) also requires the calculation of the second variation of the action. There is a relation between this quantity and the “monodromy matrix” \mathcal{M} of the characteristic trajectory which enables its numerical determination. Let $\delta u'$, $\delta u''$, $\delta v'$ and $\delta v''$ be small displacements from a given trajectory ($\delta T = 0$); then, according to (9)

$$\begin{pmatrix} \delta u'' \\ \delta v'' \end{pmatrix} = \begin{pmatrix} \frac{i}{\hbar} [S_{uv} - S_{uu} S_{vv} S_{uw}^{-1}] & S_{uv} S_{uw}^{-1} \\ -S_{uu} S_{uw}^{-1} & -i\hbar S_{uw}^{-1} \end{pmatrix} \begin{pmatrix} \delta u' \\ \delta v' \end{pmatrix} \equiv \tilde{\mathcal{M}} \begin{pmatrix} \delta u' \\ \delta v' \end{pmatrix}, \quad (32)$$

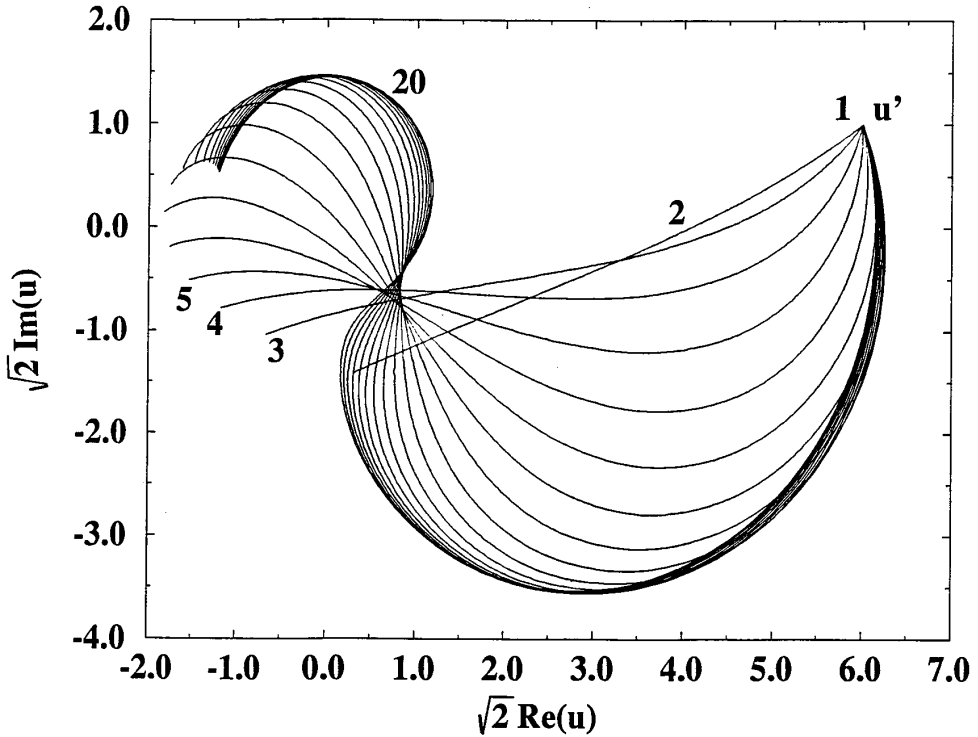


FIG. 2. Sequence of diagonal complex trajectories with $q' = q'' = 6.0$, $M = 20$, and $p' = p'' = 1.0$ between the times $T_0 = 0.001$ and $T_F = 4.0$ ($\lambda = 0$, $\beta = 0.2$).

where

$$S_{uu} = \frac{\partial^2 S}{\partial u'^2}, \quad S_{uv} = \frac{\partial^2 S}{\partial u' \partial u''}, \quad S_{vv} = \frac{\partial^2 S}{\partial v''^2}. \quad (33)$$

Therefore,

$$\frac{\partial^2 S}{\partial u' \partial v''} = i\hbar (\tilde{\mathcal{M}}_{vv})^{-1}, \quad (34)$$

where $\tilde{\mathcal{M}}_{vv}$ is the lower right element of $\tilde{\mathcal{M}}$.

The matrix $\tilde{\mathcal{M}}$ is connected to the 4×4 matrix \mathcal{M} , whose elements are m_{ij} , by Eq. (11). Notice that, since $\tilde{\mathcal{M}}$ is a complex 2×2 matrix, it has 8 elements so that among the 16 elements of \mathcal{M} only 8 are independent. A simple calculation shows that

$$\mathcal{M} = \begin{pmatrix} m_{11} & m_{12} & m_{13} & m_{14} \\ m_{21} & m_{22} & m_{23} & m_{24} \\ m_{24} & -m_{23} & m_{22} & -m_{21} \\ -m_{14} & m_{13} & -m_{12} & m_{11} \end{pmatrix}, \tag{35}$$

and

$$\Re(\tilde{\mathcal{M}}_{vv}) = \frac{1}{2} \left[m_{11} + m_{22} + \frac{c}{b} m_{12} + \frac{b}{c} m_{21} \right], \tag{36}$$

$$\Im(\tilde{\mathcal{M}}_{vv}) = -\frac{1}{2} \left[m_{14} - m_{23} + \frac{b}{c} m_{24} - \frac{c}{b} m_{13} \right].$$

Since \mathcal{M} is a by-product of the numerical method just described, we can compute the semiclassical approximation (7) completely.

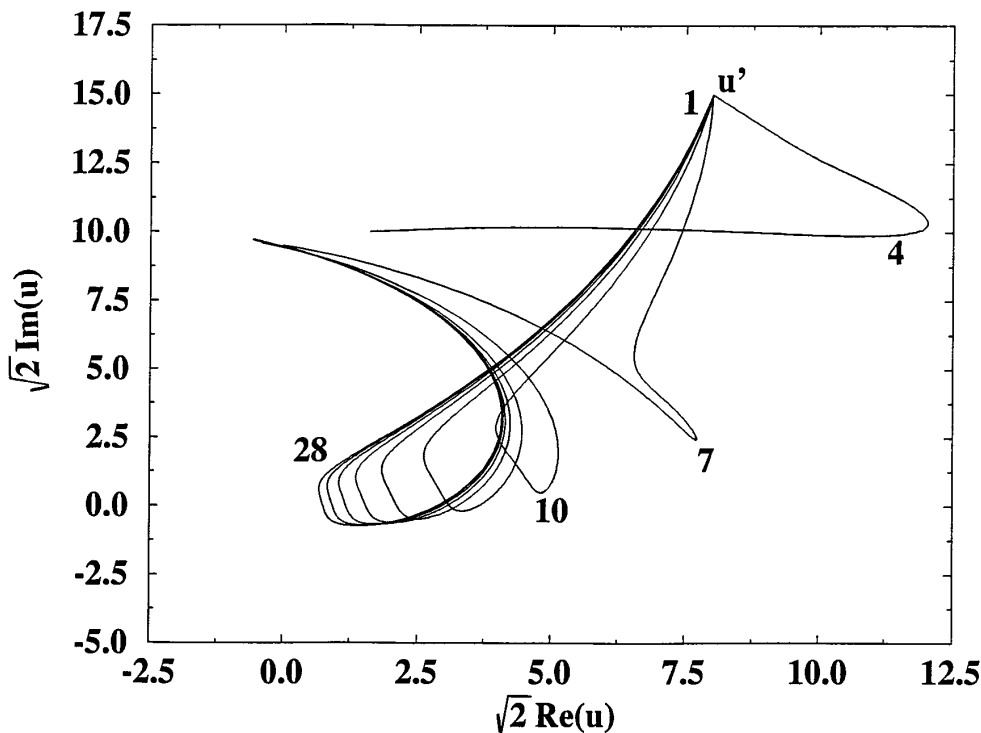


FIG. 3. Sequence of 10 diagonal complex trajectories (first family from a set of 30 trajectories) for $q' = q'' = 8.0$, $p' = p'' = 15.0$, $M = 30$ with $T_0 = 0.0001$ and $T_F = 5.5$ ($\lambda = 0$, $\beta = 0.2$).

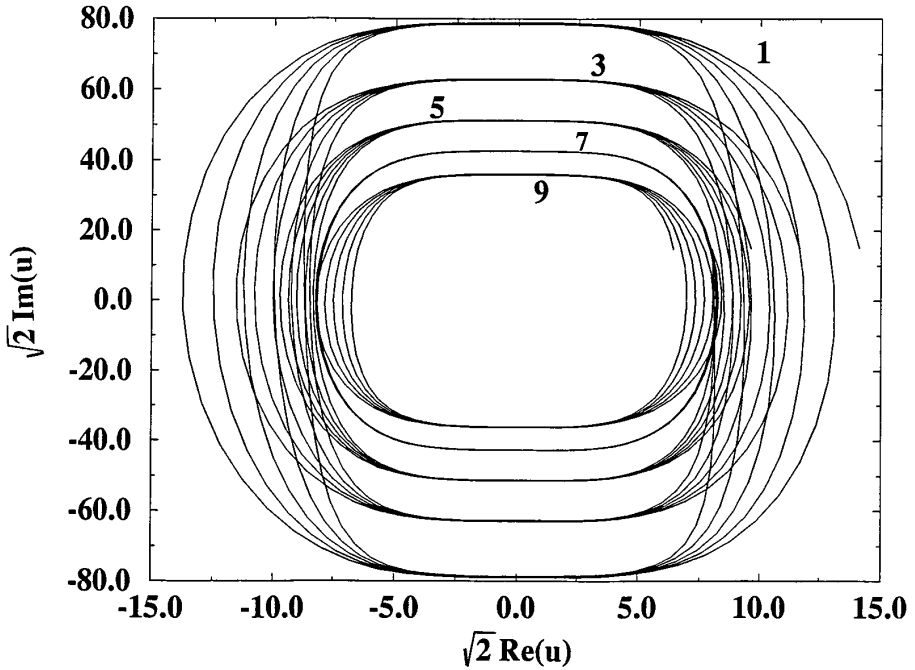


FIG. 4. Sequence of 5 diagonal complex trajectories from a set of 10 ($M=10$, family determined from the real guess) which satisfy the same boundary conditions as in Fig. 3, but with $T_0=3.5$ and $T_F=5.5$. These trajectories are very close to the corresponding real orbits ($\lambda=0$, $\beta=0.2$).

4. NUMERICAL APPLICATION

In this section we apply the method developed above to compute complex classical trajectories and the semiclassical propagator for the system described by

$$H = \frac{1}{2} p^2 + \frac{\lambda}{2} q^2 + \beta q^4, \quad (37)$$

with $\lambda \geq 0$ and $\beta > 0$. In the coordinates given by (11) the real Hamiltonian is

$$H_1 = \frac{1}{2} p_1^2 + \frac{\lambda}{2} x_1^2 - \frac{\lambda}{2} p_2^2 - \frac{1}{2} x_2^2 + \beta(x_1^4 + p_2^4 - 6x_1^2 p_2^2). \quad (38)$$

Figures 1–5 show a sequence of several complex trajectories in the $\sqrt{2} \Re(u) - \sqrt{2} \Im(u)$ plane for several values of T . In each of these figures we show the trajectories with fixed values of q' , q'' , p' , p'' , and time

$$T_j = T_0 + (T_F - T_0) \frac{(j-1)}{(M-1)}, \quad (39)$$

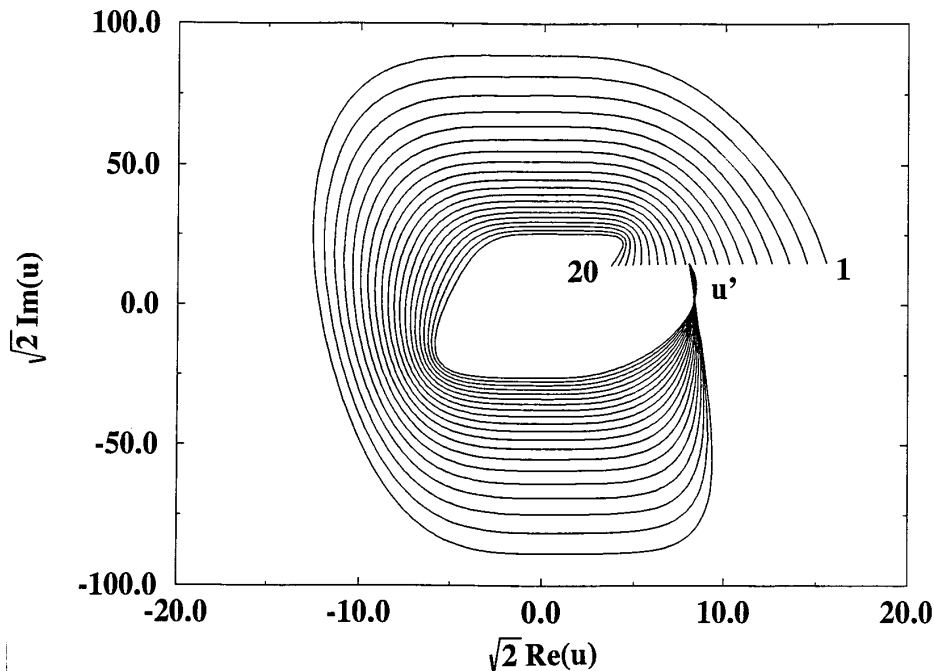


FIG. 5. Sequence of complex diagonal trajectories satisfying $q' = q'' = 8.0$, $p' = p'' = 15.0$, and $M = 20$ between $T_0 = 0.7$ and $T_F = 1.3$. The real solution is for $T = 1.003$ ($\lambda = 0$, $\beta = 0.2$).

for the j th trajectory ($j = 1, \dots, M$, the value of j is represented on each figure by a number). In these calculations we have used $h = 1$ and also $c = 1$, but $\lambda = 0$ and $\beta = 0.2$. Figure 1 shows examples of non-diagonal trajectories in which $q' = -8.0$, $q'' = 0.0$, $p' = 5.9$, $p'' = 7.9$. The 15 trajectories showed are from $T_0 = 0.0001$ to $T_F = 4.5$. The first orbit ($j = 1$) was calculated using a harmonic oscillator trajectory as the initial guess. The next trajectory ($j = 2$), in its turn, uses the $j = 1$ trajectory as the initial guess and so on. This procedure allows the computation of the whole family very easily. Figure 2 represents a sequence of 20 diagonal orbits for which $q' = q'' = 6.0$, $p' = p'' = 1.0$, $T_0 = 0.0001$, and $T_F = 4.0$. The initial guess was again provided by the harmonic oscillator. Figure 3 represents a family of 10 diagonal trajectories from a set of 30 ($M = 30$) for $q' = q'' = 8.0$, $p' = p'' = 15.0$, $T_0 = 0.0001$, $T_F = 5.5$, and initial guess from a harmonic oscillator trajectory. In Fig. 4 there is a family of 5 trajectories from a set of 10 ($M = 10$) satisfying the same boundary conditions as in Fig. 3 with $T_0 = 3.5$, $T_F = 5.5$, and each trajectory was calculated from an initial guess provides by a real periodic orbit of H through $q = 0.8$ and $p = 15.0$. The difference between both kinds of solutions is best seen by the imaginary part of the action. For periods $T \simeq 4.8$, a complex trajectory ($j = 26$) calculated from the harmonic oscillator (Fig. 3) gives $S_2 \simeq 123.0$ while, for one of

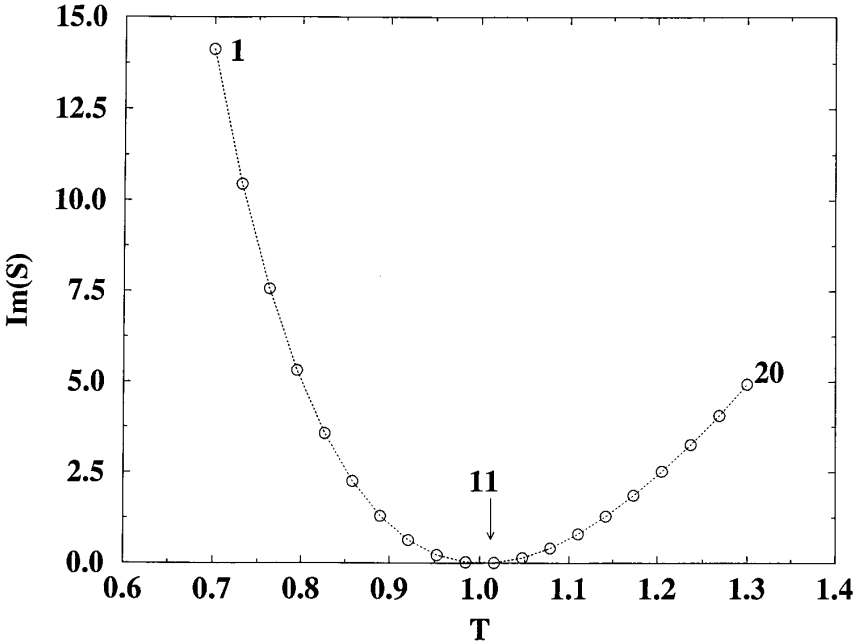


FIG. 6. $S_2(T)$ plot for the trajectories of Fig. 5. The trajectory with $j=11$ is the closest one to the real orbit ($T=1.003$) for which $S_2=0$.

the trajectories ($j=4$) of the family determined from the real quartic orbit (Fig. 4), $S_2 \simeq 0.08$. Although both trajectories satisfy the same boundary conditions, they give very different contributions for the propagator as seen from (7).

In Fig. 5 a sequence of 20 diagonal complex trajectories obtained from a periodic orbit initial guess is depicted for the conditions $q' = q'' = 8.0$, $p' = p'' = 15.0$, $T_0 = 0.7$, and $T_F = 1.3$. There is a real solution here for $\tau = 1.003$ which corresponds to a closed trajectory in the complex phase space. As we move from orbit to orbit the imaginary part of the action goes through a minimum as is seen in Fig. 6. The minimum ($S_2 = 0$) is attained at the periodic (real) orbit with $T = \tau$. Consequently the amplitude of the propagator $|\langle q'', p'' | q', p', T \rangle|^2$ at this point experiences a maximum. This will be valid for the whole phase space, i.e., the amplitude will be a maximum for every phase space point localized at a periodic orbit with period τ commensurable with the time T .

Before proceeding to the determination of $K_{scf}(z'', z', T)$, let us briefly describe how the exact propagator is computed. We write the spectral decomposition

$$K(z'', z', T) = \sum_{n=1}^{\infty} \langle z'' | n \rangle \langle n | z' \rangle e^{-iE_n T/\hbar}, \quad (40)$$

where $|n\rangle$ represents an eigenstate of H with eigenvalue E_n . The overlap $\langle n|z\rangle$ is determined by

$$\langle n|z\rangle = \left(\frac{1}{\sqrt{\pi} b}\right)^{-1/2} \int_{-\infty}^{\infty} \langle n|x\rangle \exp\left[-\frac{(x-q)^2}{4b^2} + \frac{i}{h} p(x-q/2)\right] dx, \quad (41)$$

and it constitutes the Bargmann wave function [11] of the eigenstate $\Psi_n(x) = \langle n|x\rangle$. These eigenstates are computed numerically by diagonalizing the Hamiltonian in the basis

$$\varphi_m(x) = \sqrt{\frac{1}{L}} \sin\left[m\pi\left(\frac{x}{2L} - \frac{1}{2}\right)\right], \quad (42)$$

where the parameter L is chosen according to the method described in Ref. [12]. We have used 250 basis states φ_n and obtained around 150 eigenstates Ψ_n with very good accuracy.

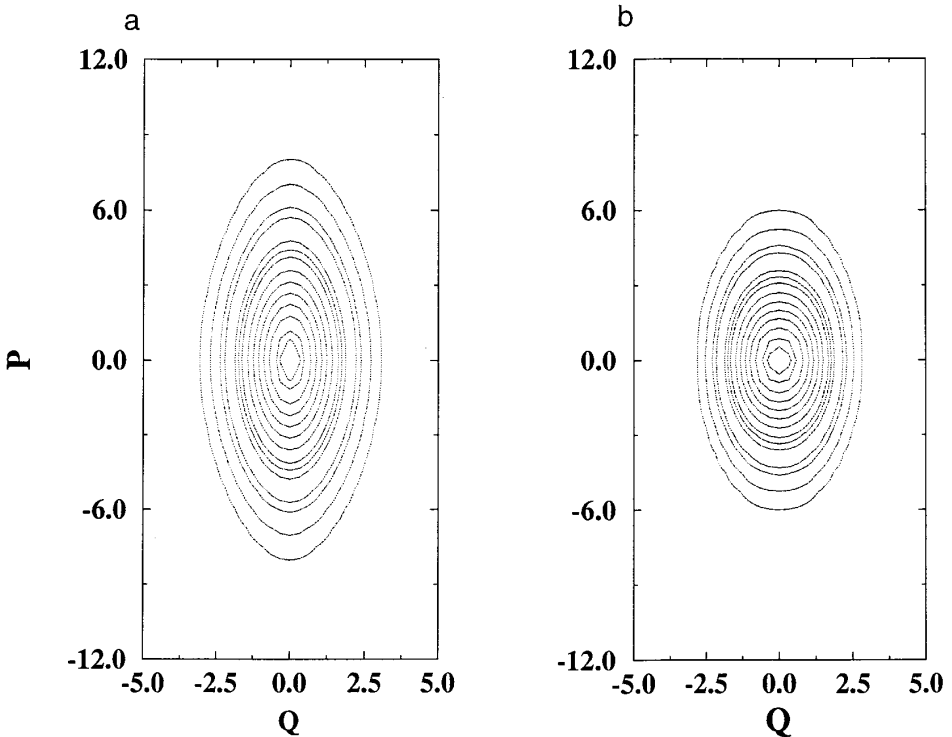


FIG. 7. Countour plots of $|K(z^*, z, T)|^2$ (normalized) for $T=0.5$: (a) quantum calculation, (b) semiclassical method ($\lambda=1.0$ and $\beta=0.1$).

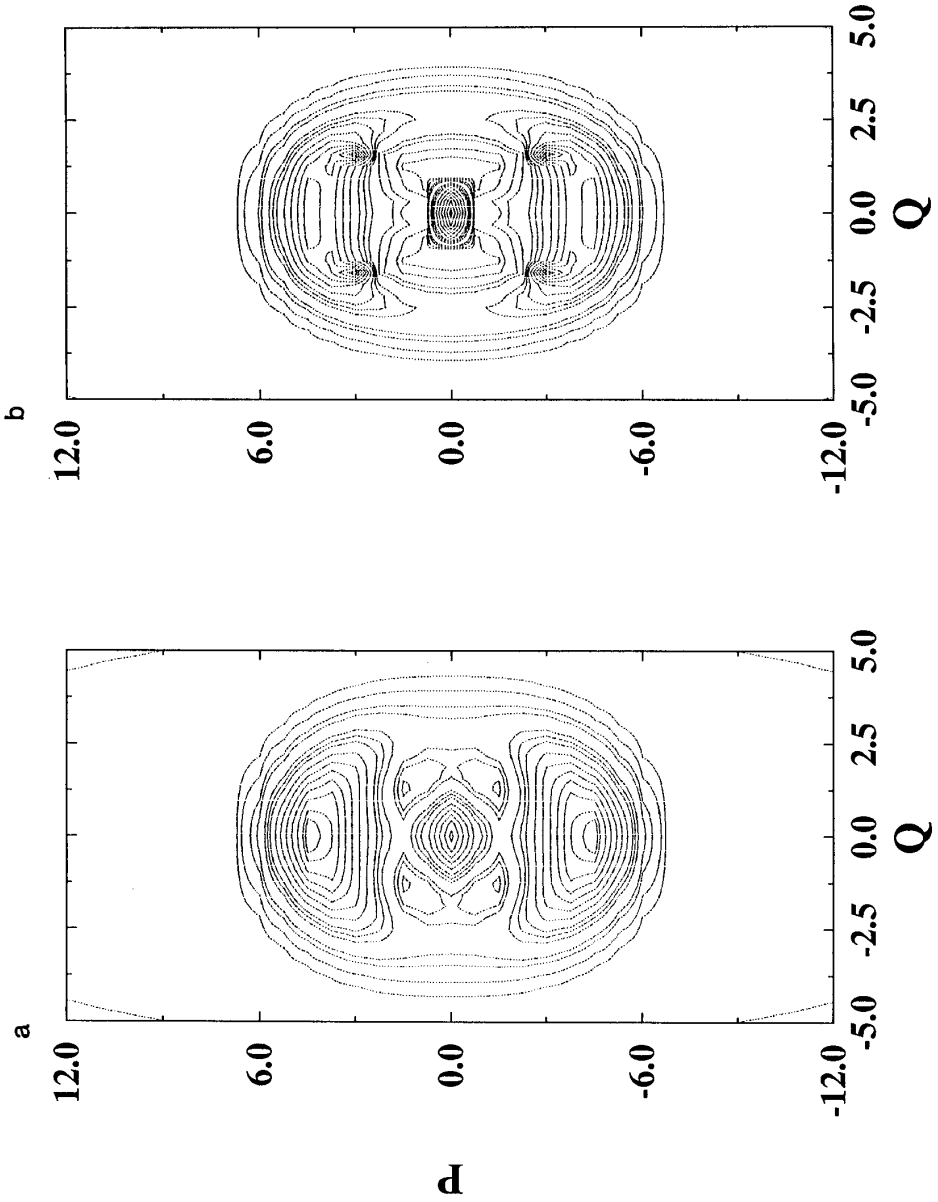


FIG. 8. Countour plots of $|K(z^*, z, T)|^2$ (normalized) for $T = 3.5$: (a) quantum calculation, (b) semiclassical method ($\lambda = 1.0$ and $\beta = 0.1$).

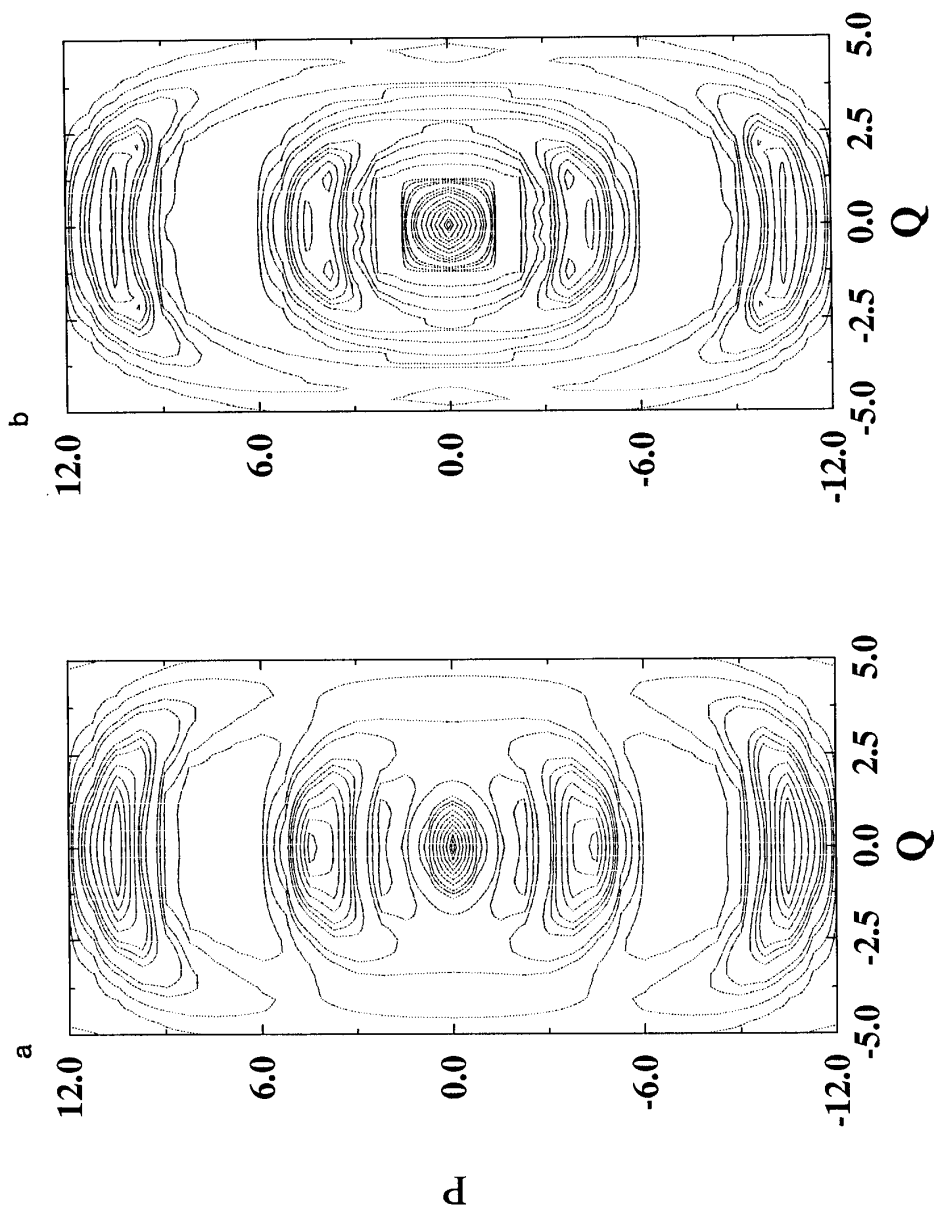


FIG. 9. Countour plots of $|K(z^*, z, T)|^2$ (normalized) for $T = 7.0$: (a) quantum calculation, (b) semiclassical method ($\lambda = 1.0$ and $\beta = 0.1$).

The sum over n in the exact propagator given by (40) was truncated at $n=100 \equiv \bar{N}$. The convergence is inferred by the value of $|K(z^*, z, 0)|^2$ which remains close to one at all phase space points. In other words

$$K(z, z, 0) \simeq \sum_{n=1}^{\bar{N}} \langle z|n\rangle \langle n|z\rangle = 1 - \sigma, \quad (43)$$

with $\sigma \approx 0$. Since the time evolution of a quantum state is linear, the difference between the time evolved truncated propagator and its complete expansion (40) will never exceed the measure given by σ .

In Figs. 7-9 we show a sequence of isoprobability curve plots of $|K(q, p, q, p, T)|^2$ (diagonal elements) calculated according to the semiclassical method (b) and the exact case (a). In these calculations the parameters in the Hamiltonian (37) have values $\lambda = 1.0$ and $\beta = 0.1$ (with again $\hbar = 1.0$ and $c = 1.0$). In all figures a sequence of 16 equally spaced curves between the values 0 and 1 are shown. For each point in the phase space in the case (b) a complex diagonal orbit was determined and its weight in the propagator was calculated. The same

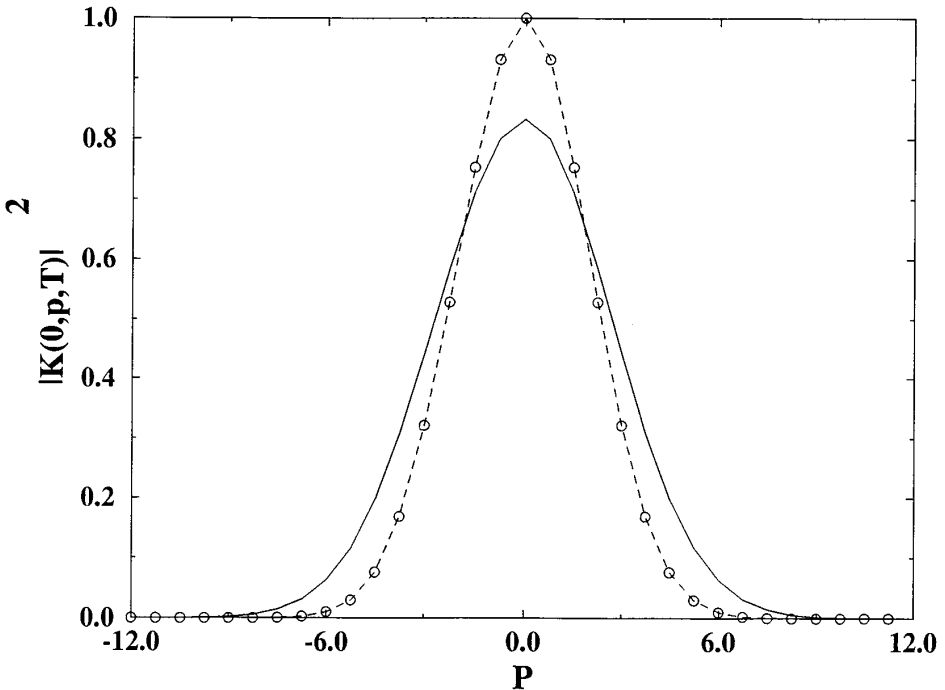


FIG. 10. $|K(z^*, z, T)|^2$ at $q=0.0$ for $T=0.5$. The solid represents the quantum calculation and the circle-dashed line the semiclassical approximation ($\lambda=1.0$ and $\beta=0.1$).

probability is shown in (a) as determined by the eigenfunction decomposition. The agreement between (a) and (b) is excellent for a broad range of values of T . In Fig. 7 ($T=0.5$), the phase space maps exhibit a maximum at the origin. As $T \rightarrow 0$ the area of the most exterior curve (minimum) grows infinitely and for every phase space point the amplitude is very close to one, as it should be ($|K(q, p, q, p, 0)|^2 = 1$). From the semiclassical point of view, as $T \rightarrow 0$, the only complex trajectories are free-particle-like solutions. Note that for a semiclassical method based entirely on ordinary (non-complex) trajectories the amplitude for diagonal elements with $p \simeq 0$ would be zero since there is no possible real trajectory that satisfies the boundary conditions required. In Figs. 8 and 9 the case $T=3.5$ and $T=7.0$ are shown. Again the agreement is excellent. We can note regions of local maxima around periodic orbits. In fact, for every periodic trajectory characterized by a period τ which is commensurable with the time T of the propagator, a maximum is expected as a consequence of the constructive interference between the initial and final wave-packet. In Figs. 10–12 we show absolute curves of amplitudes at the line $q=0$ and for the times $T=0.5$ (Fig. 10), $T=3.5$ (Fig. 11), and $T=7.0$ (Fig. 12). Dashed-lines represent the semiclassical results while solid-lines the eigenfunction decomposition. The plots show that there is also good agreement

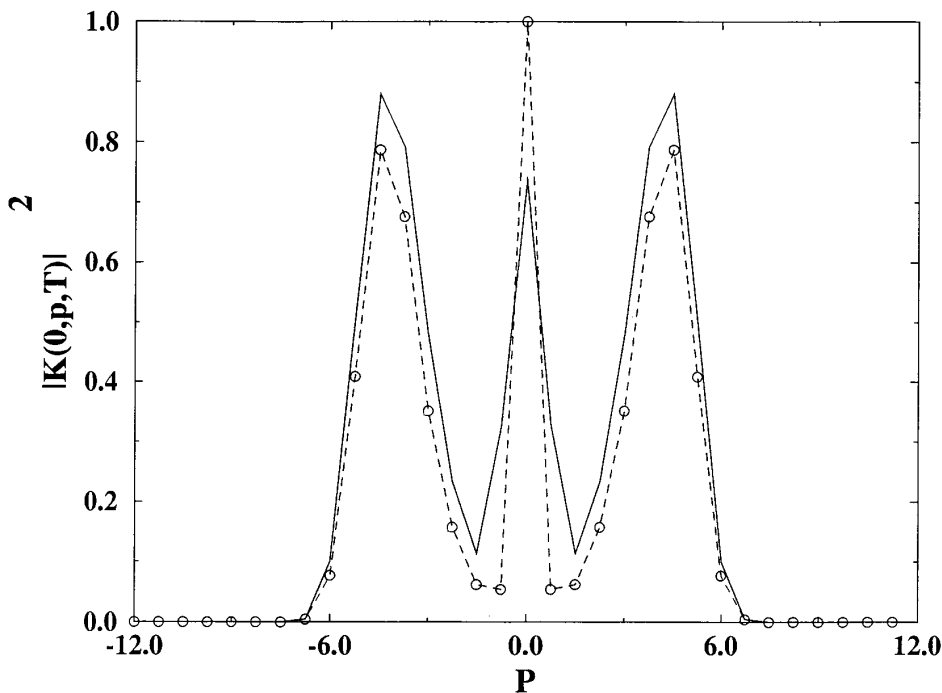


FIG. 11. $|K(z^*, z, T)|^2$ at $q=0.0$ for $T=3.5$. The solid represents the quantum calculation and the circle-dashed line the semiclassical approximation ($\lambda=1.0$ and $\beta=0.1$).

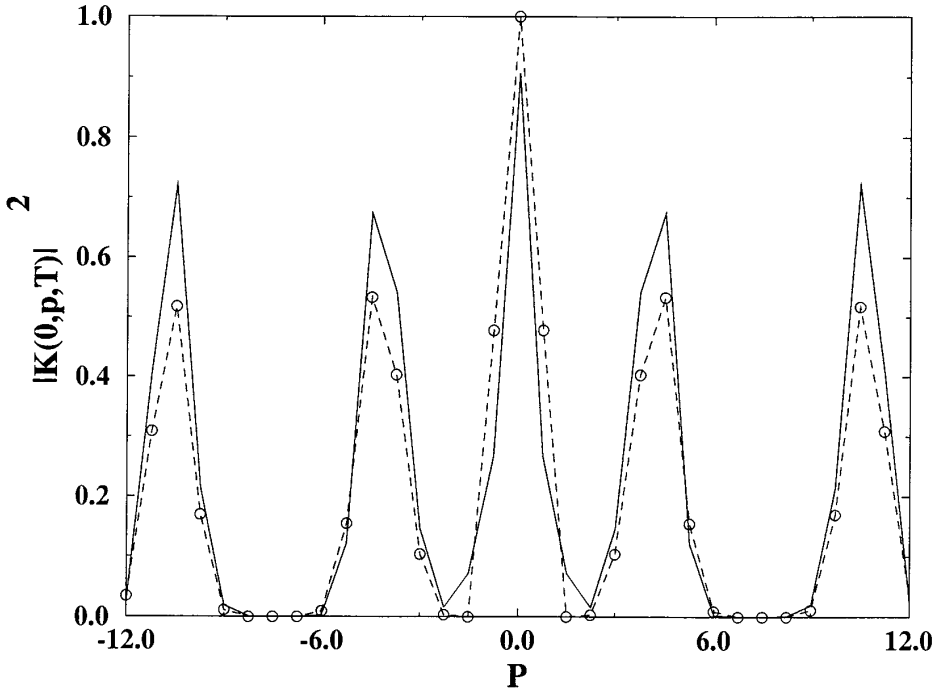


FIG. 12. $|K(z^*, z, T)|^2$ at $q=0.0$ for $T=7.0$. The solid represents the quantum calculation and the circle-dashed line the semiclassical approximation ($\lambda=1.0$ and $\beta=0.1$).

between the absolute squares of $|K(q, p, q, p, T)|^2$ as determined by the two methods. As $T \rightarrow \infty$ the density of periodic orbits increases proportionally. Therefore it will always be possible to find a periodic orbit at a point (q, p, τ) which is nearly commensurable with T .

5. DISCUSSION

We have presented a general method for computing complex trajectories subjected to the special boundary conditions required by the semiclassical coherent-state propagator $K(z'', z', T)$.

The method was applied to a quartic potential, Eq. (37), and several families of such trajectories were computed.

A previous example of semiclassical evaluation of $K(z'', z', T)$ has been considered in Ref. [7] for the problem of a particle in a one-dimensional box. In that case, due to the simplicity of the Hamiltonian, the complex trajectories could be determined analytically. One of the most interesting results in Ref. [7] is the

absence of “diagonal” trajectories (with $q' = q''$ and $p' = p''$) in several regions of the phase space, yielding $K_{scl}(z, z, T) = 0$ there.

In the present case of the quartic potential no such regions were found: for every phase space point q, p and T we were able to find at least one complex trajectory satisfying conditions (6). In some cases more than one trajectory was found, but only one of them would contribute significantly to the propagator. We attribute this fact to the smoothness of the potential.

Another interesting point in connection to the results in Ref. [7] is the seeming absence, for the quartic potential, of the so called “noncontributing trajectories”, i.e., complex trajectories whose imaginary part of the action, S_2 , is negative. As discussed in [7], these trajectories give non-physical contributions to approximation of K and should not be taken into account. For the particle-in-a-box system, these trajectories were concentrated on a thin (the thickness actually depends on T) phase space strip around $p = 0$. In the present situation, the dynamics in regions around $p = 0$ is essentially harmonic and, in this case, it is easy to show that $S_2 > 0$. At higher values of p (or higher energies) the quartic term dominates, and the dynamics become similar to that of the particle-in-a-box. In the present case, however, noncontributing orbits were not found. That does not mean, of course, that they do not exist, but it indicates that, if they exist then they are deeply buried in the complex plane, far from our search region.

The results we have obtained for the propagator show a strong agreement between the amplitude determined by its eigenfunctions decomposition (exact quantum result) and by the semiclassical formula. The great value of this semiclassical method lies in its ability to determine the overlap between coherent-states for which there is no real trajectory available. Tunnelling is perhaps the most dramatic example where the existence of “trajectories,” in spite of their being complex, would enable the definition of tunnelling times. Results in this direction will be published elsewhere in the future.

ACKNOWLEDGMENTS

The authors acknowledge financial support from CNP_q, FAPESP, and FINEP. One of the authors (ALXJ) especially acknowledges support from FAPESP under Contract 93/2490-0.

REFERENCES

1. J. R. Klauder, in “Path Integrals, Proceedings of the NATO Advanced Study Institute” (G. J. Papadopoulos and J. T. Devreese, Eds.), p. 5, Plenum, New York, 1978.
2. J. R. Klauder, *Phys. Rev. D* **19** (1979), 2349.
3. Y. Weissman, *J. Phys. A* **16** (1983), 2693.
4. S. Adachi, *Ann. Phys.* **195** (1989), 45.
5. A. Robin and J. R. Klauder, *Ann. Phys.* **241** (1995), 212.

6. D. W. McLaughlin, *J. Math. Phys.* **13** (1972), 1099.
7. A. L. Xavier Jr. and M. A. M. de Aguiar, *Phys. Rev. A*, to appear.
8. M. Baranger, K. T. R. Davies, and J. H. Mahoney, *Ann. Phys.* **186** (1988), 95.
9. M. A. M. de Aguiar and M. Baranger, unpublished.
10. N. Bleistein and R. A. Handelsmann, "Asymptotic Expansions of Integrals," Dover, New York, 1969.
11. V. Bargmann, *Comm. Pure Appl. Math.* **14** (1961), 187.
12. M. A. M. de Aguiar and A. L. Xavier Jr., *Phys. Lett. A* **164** (1992), 279.